The American Journal of Pathology, Vol. 192, No. 7, July 2022

ELSEVIER

The American Journal of
PATHOLOGY
ajp.amjpathol.org

CARDIOVASCULAR, PULMONARY, AND RENAL PATHOLOGY

Angiopoietin 2 Is Associated with Vascular Necroptosis Induction in Coronavirus Disease 2019 Acute Respiratory Distress Syndrome

David R. Price,[*†] Elisa Benedetti,[‡] Katherine L. Hoffman,[§] Luis Gomez-Escobar,[*] Sergio Alvarez-Mulett,[*] Allyson Capili,[*] Hina Sarwath,[¶] Christopher N. Parkhurst,[*†] Elyse Lafond,[*†] Karissa Weidman,[*†] Arjun Ravishankar,[‖] Jin Gyu Cheong,[‖] Richa Batra,[‡] Mustafa Büyüközkan,[‡] Kelsey Chetnik,[‡] Imaani Easthausen,[§] Edward J. Schenck,[*†] Alexandra C. Racanelli,[*†] Hasina Outtz Reed,[*†] Jeffrey Laurence,[†**] Steven Z. Josefowicz,[‖] Lindsay Lief,[*†] Mary E. Choi,[†,††] Frank Schmidt,[¶] Alain C. Borczuk,[‡‡] Augustine M.K. Choi,[*†] Jan Krumsiek,[‡] and Shahin Rafii[†§§]

From the Division of Pulmonary and Critical Care Medicine, Department of Medicine, New York-Presbyterian Hospital—Weill Cornell Medical Center, the Institute of Computational Biomedicine,[‡] Department of Physiology and Biophysics, the Division of Biostatistics,[§] Department of Population Health Sciences, the Laboratory of Epigenetics and Immunity,[‖] Department of Pathology and Laboratory Medicine, the Divisions of Hematology and Medical Oncology** and Nephrology and Hypertension,[††] Department of Medicine, and the Ansary Stem Cell Institute,[§§] Division of Regenerative Medicine, Department of Medicine; Weill Cornell Medicine, New York, New York; the Department of Medicine,[†] New York-Presbyterian Hospital—Weill Cornell Medical Center, New York, New York; the Proteomics Core,[¶] Weill Cornell Medicine-Qatar, Qatar Foundation-Education City, Doha, Qatar; and the Department of Pathology and Laboratory Medicine,[‡‡] New York Presbyterian—Weill Cornell Medicine, New York, New York*

Accepted for publication April 4, 2022.

Address correspondence to Jan Krumsiek, Ph.D., or Shahin Rafii, M.D., Weill Cornell Medicine, 1305 York Ave., New York, NY 10021. E-mail: jak2043@med.cornell.edu or srafii@med.cornell.edu.

Vascular injury is a well-established, disease-modifying factor in acute respiratory distress syndrome (ARDS) pathogenesis. Recently, coronavirus disease 2019 (COVID-19)—induced injury to the vascular compartment has been linked to complement activation, microvascular thrombosis, and dysregulated immune responses. This study sought to assess whether aberrant vascular activation in this prothrombotic context was associated with the induction of necroptotic vascular cell death. To achieve this, proteomic analysis was performed on blood samples from COVID-19 subjects at distinct time points during ARDS pathogenesis (hospitalized at risk, $N = 59$; ARDS, $N = 31$; and recovery, $N = 12$). Assessment of circulating vascular markers in the at-risk cohort revealed a signature of low vascular protein abundance that tracked with low platelet levels and increased mortality. This signature was replicated in the ARDS cohort and correlated with increased plasma angiopoietin 2 levels. COVID-19 ARDS lung autopsy immunostaining confirmed a link between vascular injury (angiopoietin 2) and platelet-rich microthrombi (CD61) and induction of necrotic cell death [phosphorylated mixed lineage kinase domain-like (pMLKL)]. Among recovery subjects, the vascular signature identified patients with poor functional outcomes. Taken together, this vascular injury signature was associated with low platelet levels and increased mortality and can be used to identify ARDS patients most likely to benefit from vascular targeted therapies. *(Am J Pathol 2022, 192: 1001—1015; https://doi.org/10.1016/j.ajpath.2022.04.002)*

Supported by the Biomedical Research Program at Weill Cornell Medicine in Qatar, a program funded by the Qatar Foundation; the NIH National Institute of Aging award 1U19AG063744 (J.K.); the NIH National Heart, Lung, and Blood Institute grant T32HL134629-01A1 (D.R.P.); and Stony Wold-Herbert Fellowship Fund (United States; D.R.P.).

D.R.P. and E.B. share first authorship.

J.K. and S.R. share last authorship.

Disclosures: A.M.K.C. is a cofounder, is a stock holder, and serves on the Scientific Advisory Board for Proterris, which develops therapeutic uses for carbon monoxide. A.M.K.C. also has a use patent on carbon monoxide. The spouse of M.E.C. is a cofounder and shareholder and serves on the Scientific Advisory Board of Proterris, Inc. E.J.S. reports consulting fees from Axle Informatics for work assisting National Institute of Allergy and Infectious Diseases with coronavirus disease 2019—related vaccine clinical trials. All other authors declare no competing interest.

https://doi.org/10.1016/j.ajpath.2022.04.002

For decades, vascular injury has been recognized as a key element in the pathogenesis of acute respiratory distress syndrome (ARDS).[1] However, this has not translated into vascular targeted therapies for ARDS. This may, in part, be related to heterogeneity in the vascular response to injury among ARDS subjects, as well as to difficulty in selecting patients most at risk for ARDS vascular injury. Blood proteomics has been proposed as a novel translational approach to better match patients to precision therapies for ARDS.[2] A better understanding of the blood proteomic changes associated with ARDS vascular injury could therefore help identify patients likely to benefit from vascular therapies.

Previous targeted studies of circulating vascular proteins have greatly enhanced the understanding of ARDS vascular injury. For example, measurement of the plasma angiocrine factor angiopoietin 2 (ANGPT2) in patients at the early stages of ARDS demonstrates that vascular injury likely precedes mechanical ventilation[3] and is associated with ARDS disease mortality.[4] However, these ANGPT2-mediated vascular disruptions can be countered. In mice, systemic administration of platelet-derived pericyte chemokines, such as angiopoietin 1 (ANGPT1) and platelet-derived growth factor B (PDGFB), counter ANGPT2-mediated vascular disruption, demonstrating the homeostatic potential of the blood vascular proteome.[5] Improved understanding of the blood proteomic changes in subjects with ARDS with high or low vascular injury can build on these prior observations, shed further light onto disease pathogenesis, and identify protein targets for further investigation.

More recently, vascular injury has been associated with coronavirus disease 2019 (COVID-19) ARDS,[6,7] including the vascular complications of inflammation and thrombosis. In this context, COVID-19–induced injury to the vascular compartment has been associated with complement activation and microvascular thrombosis,[8–10] systemic thrombosis,[9,11] and dysregulated immune responses.[12,13] However, this focus on inflammation and thrombosis limits our insights into other disruptions associated with aberrant vascular activation, including angiogenesis, junctional barrier integrity, the role of activated platelets in vascular injury, and induction of vascular cell death, including specialized receptor-interacting protein kinase 3 (RIPK3)–mediated necrotic cell death. Specifically, although ANGPT2-mediated vascular disruption has been documented in COVID-19,[14] the association between ANGPT2 and induction of vascular cell death remains largely unexplored in ARDS investigations.

The purpose of this study was to assess whether aberrant vascular activation in COVID-19 was associated with the induction of necroptotic vascular cell death. To this aim, blood proteomics was performed in three independent COVID-19 cohorts, which enrolled patients at distinct time points in disease pathogenesis and included non–COVID-19 ARDS samples as control. Protein expression was linked to relevant clinical outcomes, vascular injury, and cell death markers in COVID-19 autopsy lung tissue.

Materials and Methods

Study Design

This study is an exploratory analysis of three cohorts that independently enrolled COVID-19 subjects at New York Presbyterian Weill Cornell Medical Center (WCM) between March 15 and August 17, 2020. Additional historic non–COVID-19 ARDS samples from influenza and bacterial ARDS patients prospectively enrolled into the Weill Cornell Biobank of Critical Illness from October 20, 2014, until May 24, 2020, were included as part of the ARDS cohort as ARDS controls. The three COVID-19 cohorts were identified according to ARDS status at enrollment, yielding an early hospitalization at-risk cohort, termed at risk; an intensive care unit (ICU) cohort with ARDS, termed ARDS; and a recovery cohort in early convalescence outside the ICU, termed recovery.

Cohort Descriptions

The at-risk cohort included 59 adult (aged >18 years) nonpregnant COVID-19 subjects admitted to the general wards of WCM with serum available and who did not meet ARDS criteria at study enrollment. The ARDS cohort included adult (aged >18 years) nonpregnant COVID-19 ($N = 31$) and historic non-COVID ARDS ($N = 29$) subjects admitted to the ICU at WCM. For the ARDS cohort, only study subjects meeting ARDS criteria and with blood sampling within 10 days of ICU admission were considered for analysis. The recovery cohort included 12 adult (aged >18 years) nonpregnant COVID-19 ARDS subjects with plasma samples available from both the time of ICU care and the subsequent recovery period to allow for longitudinal analyses.

Blood Sampling

In the at-risk cohort, between one and three consecutive daily samples were obtained from the central laboratory after routine processing to obtain serum. To obtain serum, blood collected in serum separator tubes was processed within 2 hours of venipuncture. Whole blood was centrifuged at 1500 × g for 7 minutes. The serum layer was aliquoted and stored at −80°C. These samples were obtained with a waiver of informed consent. In this cohort, samples collected after patient intubation were excluded from the analysis. In the ARDS and recovery cohorts, plasma was isolated from study subjects according to existing plasma isolation protocols.[15–18] To obtain plasma, blood collected in EDTA tubes was processed within 6 hours of venipuncture. Whole blood was centrifuged at 490

$\times g$ for 10 minutes. The plasma layer was removed in 200-μL aliquots and stored at −80°C. ARDS samples were obtained from patients in the intensive care unit, whereas recovery blood samples were obtained from patients convalescing in the hospital rehabilitation floors, as well as from the New York Presbyterian Weill Cornell Medicine Post-ICU recovery clinic.

Clinical Evaluation

Baseline clinical parameters and outcomes were extracted from the electronic medical record, as described previously.[19,20] Baseline comorbidities were manually extracted from the electronic medical record. Baseline clinical data (laboratory results, severity of illness, and ventilator data) were measured at time of blood sampling in both the at-risk cohort and ARDS cohort. In the recovery cohort, baseline clinical data were measured from the ICU time point to allow for direct comparison with the ARDS cohort. Severity of illness was defined by the Sequential Organ Failure Assessment score.[21] ARDS was determined according to the Berlin definition, with ARDS severity capped at mild for subjects on noninvasive ventilation.[22] Two critical care investigators independently adjudicated the ARDS diagnosis. In all study subjects, COVID-19 was diagnosed if a subject had a syndrome compatible with COVID-19 and a nasopharyngeal swab positive for severe acute respiratory syndrome coronavirus 2 (SARS-CoV-2) by reverse transcription PCR.

Recovery Evaluation

The EuroQol five-dimension, three-level (EQ-5D-3L) assessment was used to assess recovery at 12 months from ICU admission. The EQ-5D-3L is a self-assessment of the patient recovery, and considers five distinct domains (namely, mobility, self-care, usual activities, pain or discomfort, and anxiety or depression).[23] Each domain was scored as 0, 1, or 2, depending on whether the patient reported no, some, or extensive limitations in each respective domain. For each patient, a final score was defined as the sum of the scores across the five domains and treated as an ordinal variable in the statistical analysis. Maximal functional limitation would have a score of $2 \times 5 = 10$, whereas an optimal recovery would be scored 0.

Autopsy Studies

Twenty autopsies, performed between March 19 and June 30, 2020, with premortem nasopharyngeal swabs positive for SARS-CoV-2 were considered for lung tissue staining. Hematoxylin and eosin, ANGPT2, CD61, and phosphorylated mixed lineage kinase domain-like (pMLKL) staining were performed in all autopsy subjects. In addition, CD31 and ANGPT2/erythroblast transformation-specific-related gene (ERG) costaining were performed on the four autopsy subjects highlighted in the article.

All autopsies were performed in a negative pressure ventilation room with full personal protective equipment, including N-95 masks. No bone saw was used to prevent aerosolized dusts and, as such, brain examination was not performed. All tissues were immediately fixed in formalin for a minimum of 24 hours. To minimize exposure, only two individuals were allowed in the suite during the autopsy, and the room was disinfected before and after each case. Lung tissue specimens were fixed in 10% formalin for 48 to 72 hours. Hematoxylin and eosin staining was performed for all cases. Immunohistochemistry was performed for ANGPT2 (sc-74403; Santa Cruz Biotechnology, Dallas, TX; 1:100), CD61 (CD61 clone 2F2; Leica Biosystems, Deer Park, IL), ERG (ab92513; Abcam, Cambridge, UK; 1:100), CD31 (PA0250; Leica Biosystems; ready to use), and pMLKL (MAB91871; Novus Biologicals, Centennial, CO; 1:750 with casein for background reduction). Specimens were scanned by whole-slide image technique using an Aperio slide scanner (Leica Biosystems) with a resolution of 0.24 μm per pixel. Quantification of ANGPT2 and CD61 was performed on four random ×20 images selected using a random overlay of points and excluding fields with large vessels or airway. All 20 autopsies were analyzed using Immunohistochemistry profiler[24] as a plugin for ImageJ software version 1.52a (NIH, Bethesda, MD; *https://imagej.nih.gov*, last accessed March 10, 2022). After deconvolution of the ×20 images, both area of expression (eg, number of pixels) and intensity of expression (eg, intensity of pixel) were measured and combined into a single score, according to the equation score = (number of pixels in a zone × score of the zone)/total number of pixels in image. High, intermediate, low, and overall percentage positive were averaged over the four measurements. The median ANGPT2 quantification was used to define the high (greater than median) and low (less than median) ANGPT2 staining. The association between CD61 and ANGPT2 was then calculated on the basis of CD61 quantification in the low and high ANGPT2 groups using *U*-test.

O-link Plasma Proteomics

To quantify the circulating vascular proteome, plasma and serum samples from the at-risk, ARDS, and recovery cohorts were profiled using O-link through the Proteomics Core of Weill Cornell Medicine-Qatar. The O-link assays were performed using Inflammation version 3021, Cardiovascular II version 5005, and Cardiovascular III version 6113 panels (O-link, Uppsala, Sweden).

EDTA plasma and serum samples were heat inactivated at 56°C for 15 minutes. The protein measurements were performed with the Proximity Extension Assay technology, according to manufacturer's instructions. In summary, high-throughput real-time PCR of reporter DNA linked to protein-specific antibodies was performed on a 96-well

integrated fluidic circuits chip (Fluidigm, San Francisco, CA). Signal quantification was performed on a Biomark HD system (Fluidigm, San Francisco, CA). Each sample was spiked with quality controls to monitor the incubation, extension, and detection steps of the assay. In addition, samples representing external, negative, and interplate controls were included in each analysis run. From raw data, real-time PCR C_T values were extracted using the Fluidigm real-time PCR analysis software version 4.5.2 at a quality threshold of 0.5 and linear baseline correction. C_T values were further processed using the O-link NPX manager software version 5.0 (O-link). Herein, log2-transformed C_T values from each sample and analyte were normalized on the basis of spiked-in extension controls and scale inverted to obtain normalized log2 scaled protein expression values. Normalized log2 scaled protein expression values were further adjusted on the basis of the median of interplate controls for each protein and intensity median scaled between all samples and plates. As an external validation of the O-link platform, plasma protein levels of CD40 ligand (CD40LG) and ANGPT1 were measure by enzyme-linked immunosorbent assays (ELISAs; see section below) in high and low expression patient samples and correlation measured between O-link and ELISA protein values.

The at-risk cohort was profiled in two separate runs. The second run included a total of 11 samples, among which 5 bridge samples were used to scale this batch toward the first one, as recommended by O-link. First, for each bridge sample, the pairwise difference between the first and second batch was computed. An overall batch adjustment factor was then derived as the median of these pairwise differences and subtracted to the values in the second batch.

Subsequently, protein levels were exponentiated, normalized using probabilistic quotient normalization,[25] and log2 retransformed. Missing values were imputed using a k-nearest neighbors approach[26] ($k = 10$). A total of 10 proteins were measured across multiple panels and, therefore, their duplicated values were averaged, leaving a total of 266 unique proteins. Protein values were standardized before statistical analysis. The preprocessed O-link and validation ELISA proteomics data for the three cohorts presented in this article are available (*https://doi.org/10.6084/m9.figshare.19341536.v1*, last accessed March 10, 2022).

ELISA Measurements

Plasma samples from the ARDS and recovery cohorts were used for ELISAs, according to manufacturer recommendations. Human ANGPT2 (R&D Systems, Minneapolis, MN; catalog number DANG20) and RIPK3 (Cusabio, Houston, TX; catalog number CSB-EL019737HU) kits were used to measure plasma protein levels. In addition, CD40LG (R&D Systems; catalog number DCDL40) and ANGPT1 (R&D Systems; catalog number DANG10) were measured in high- and low-expressing patient samples ($N = 6$ each, 12 total) to validate the O-link platform. Plasma samples were diluted (1:8 dilution for ANGPT2, 1:10 dilution for RIPK3, 1:8 dilution for ANGPT1, and 1:15 dilution for CD40L) before plating. Final sample absorbance was measured at 450 nm with wavelength correction performed at 570 nm. Sample concentrations were calculated from a four-parameter logistic curve generated from known standard concentrations. Dilution factors were accounted for to calculate the final sample concentration. Plasma protein values were log10 transformed before statistical analysis.

Statistical Analysis

In the at-risk cohort, proteomic analysis, protein associations with death (ie, whether the patient ended up dying), and platelet count (minimum value across the sampling days) were computed using a mixed linear effect model, which allows for proper accounting of the multiple samples collected per patient. The model was formulated as follows: protein $\sim$ outcome + replicate + batch + (1|patient), where outcome is either death or platelet count, replicate indicated the day of blood sample draw (first, second, or third since hospital admission), and batch indicated whether the sample was measured in the first or second run. Association P values were corrected for multiple testing using the Benjamini-Hochberg method for controlling the false discovery rate.[27] Adjusted $P < 0.1$ was considered significant.

The protein vascular signature was selected from proteins significantly associated with both outcomes, and proteins significantly associated with either mortality or platelet count and with known, well-characterized links to vascular function. TIE2 was additionally included as it is the receptor for ANGPT2.

For all cohorts, patient hierarchical clustering based on the standardized proteomics value was performed using Ward linkage and euclidean distance. The differential analysis between patient clusters was performed using U-tests for continuous variables, Kendall rank correlation for ordinal variables, and log-rank tests for survival times. The correlation between ANGPT2 and RIPK3 was estimated using Pearson correlation. For these analyses, $P < 0.05$ was considered significant.

In the recovery cohort, patients were first divided into two groups based on unsupervised hierarchical clustering (Ward linkage, euclidean distance) performed on the recovery time point. Then, for each patient, a protein abundance difference (Δ) was calculated between the ICU and recovery time points. Finally, for each protein, it was determined whether the protein Δ was different across the two patient groups using the linear model $\Delta \sim$ group. P values were corrected for multiple tests using the Benjamini-Hochberg method. Given the small sample size and validation of protein set in two prior cohorts, an adjusted $P < 0.25$ was considered significant.

All statistical analyses were performed in R 4.0.1 using the maplet package.[28] The R code used to generate the statistical findings presented in this article is publicly

available (*https://github.com/krumsieklab/covid-vascular-injury*, last accessed March 10, 2022).

Study Approval

The study was approved by the institutional review board at WCM (20-05022072, 20-03021681, and 1811019771). Written informed consent was received before participation by all patients, except when the institutional review board approved a waiver of informed consent (eg, for the use of discarded samples and deidentified patient data in the at-risk cohort).

Results

The Hospitalized At-Risk Cohort Blood Proteome Identifies a Signature of Vascular Limitation Preceding Critical Illness

A total of 1384 subjects were admitted to the medical floors of WCM during the study period. Of the 1384 hospitalized subjects with COVID-19, 59 were profiled (Figure 1). Profiled subjects were more likely to have cancer (15% versus 7.5%; $P = 0.044$) but otherwise were similar to unprofiled subjects (Supplemental Table S1). The median age of profiled subjects in the at-risk cohort was 69 years, and was majority male (64% male versus 36% female). Of the cohort, 53% had hypertension and 15% had cancer. Additional cohort characteristics are listed in Supplemental Table S2.

Blood biomarkers in the at-risk cohort were measured using the O-link proximity extension assay. External validation of protein expression by ELISA showed excellent correlation between O-link and ELISA protein measurements: $CD40LG_{OLink}$ and $CD40LG_{ELISA}$ was $R = 0.94$ ($P < 0.001$) (Supplemental Figure S1A), and $ANGPT1_{OLink}$ and $ANGPT1_{ELISA}$ was $R = 0.94$ ($P < 0.001$) (Supplemental Figure S1B). To first identify clinically relevant proteins associated with vascular injury and platelet thrombosis, a protein set was defined on the basis of the association of circulating proteins with death and platelet levels (Figure 2A). Thirteen proteins were significantly associated with both parameters (false discovery rate, 0.1): platelet-derived growth factor subunit A (PDGFA), PDGFB, ANGPT1, sortilin 1 (SORT1), proheparin-binding EGF-like growth factor (HBEGF), latency-associated peptide transforming growth factor beta-1 (LAP TGFB1), CD84, C-X-C motif chemokine 5 (CXCL5), matrix metalloproteinase-9 (MMP9), plasminogen activator inhibitor 1 (PAI), interleukin-7 (IL7), interleukin-1 receptor antagonist (IL1RA), and C-X-C motif chemokine 1 (CXCL1). In addition, eight proteins were selected as they were associated with either death or platelet count (false discovery rate, 0.1) and have known vascular functions: a disintegrin and metalloproteinase with thrombospondin motifs 13 (ADAMTS13), CD40LG, epidermal growth factor receptor (EGFR), P-selectin (SELP), urokinase-type plasminogen activator (UPA), vascular endothelial growth factor A (VEGFA), platelet glycoprotein VI (GP6), and heme oxygenase 1 (HO1). TIE2 was additionally included because it is the receptor for ANGPT1 and ANGPT2.[29] The final set comprised of 22 proteins (Supplemental Figure S2), including proteins related to vascular junctional integrity (ANGPT1 and TIE2), angiogenesis (PDGFA and PDGFB), platelet degranulation (CD40LG and GP6), and coagulopathy (ADAMTS13 and PAI), highlighting the potential functional significance of the identified proteins. Notably, these representative vascular proteins had lower expression in at-risk subjects who died (Figure 2B), representing an early signal of vascular limitation in COVID-19 pathogenesis.

Patient clustering based on this protein set identified three distinct patient groups (clusters A, B, and C) (Figure 2C), with mortality and low platelets progressively enriched. Interestingly, this mortality and low platelet enrichment was associated with lower mean abundance of the 22 proteins ($P < 0.001$) (Supplemental Figure S3A) and older age ($P = 0.016$) (Supplemental Figure S3B). Baseline cancer status ($P = 0.043$) (Supplemental Table S3) as well as creatinine ($P = 0.011$) (Supplemental Table S3) were additionally enriched across the patient clusters, identifying additional patient characteristics associated with low protein abundance.

Loss of Circulating Vascular Proteins Is Associated with Low Platelets, Mortality, and Plasma ANGPT2 in ARDS

Next, the vascular protein signature was evaluated in the ARDS cohort. A total of 439 subjects with COVID-19 ARDS were admitted to the WCM ICUs during the study period. Thirty-one subjects with COVID-19 ARDS were profiled, together with 29 non−COVID-19 ARDS controls selected from 57 total non−COVID-19 ARDS subjects in the ICU biobank (Figure 1). Profiled subjects with COVID-19 ARDS were younger (62 versus 67 years; $P = 0.032$), but otherwise were similar to unprofiled subjects with COVID-19 ARDS (Supplemental Table S4). There were no baseline differences between profiled and unprofiled non−COVID-19 ARDS control subjects (Supplemental Table S4). Among all profiled subjects with ARDS ($N = 60$), there were no significant age, sex, or race differences between COVID-19 ARDS ($N = 31$) and non−COVID-19 ARDS subjects ($N = 29$) in the cohort (Supplemental Table S2). Cancer was overrepresented in the non−COVID-19 ARDS control subjects (48.0% versus 3.2% in COVID-19 ARDS). There were also notable differences in respiratory physiology. COVID-19 ARDS was associated with more severe hypoxemia [partial pressure of arterial oxygen:fraction of inspired oxygen (PaO2:FiO2) ratio, 84 versus 193 in non−COVID-19 ARDS] but lower ventilator ratio (1.65 versus 2.89 in non−COVID-19 ARDS).

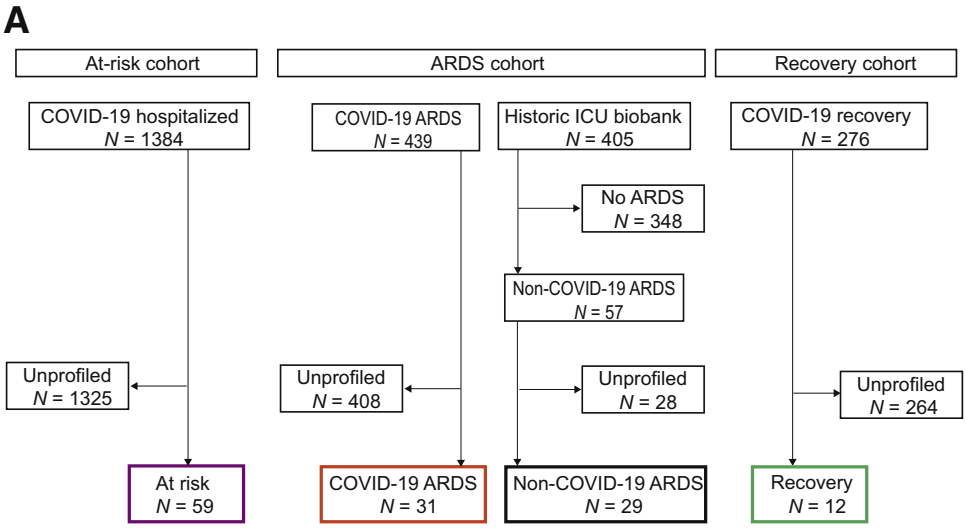

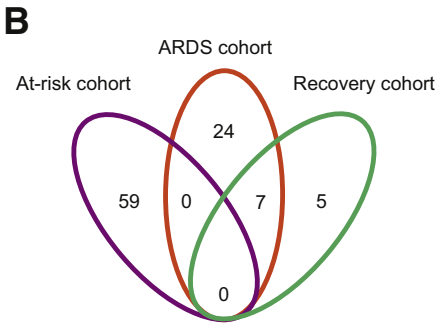

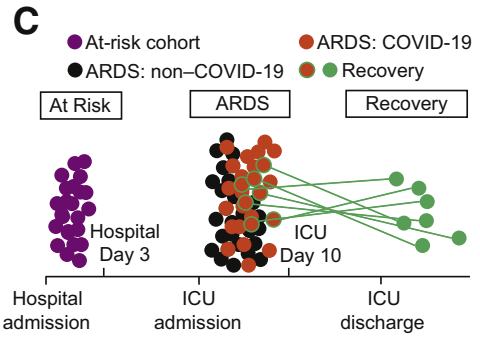

D

Cohort	*N*	Sample	Longitudinal samples	Sample timing	Proteomics	ANGPT2	RIPK3
At Risk	59	Serum	No	Hospital day 1-3	Yes	No	No
ARDS	60				Yes	Yes	Yes
COVID-19	31	Plasma	No	ICU day 1-10	Yes	Yes	Yes
Non-COVID-19	29	Plasma	No	ICU day 1-10	Yes	Yes	Yes
Recovery	12	Plasma	Yes	ICU: day 1-10 Recovery: after ICU	Yes Yes	Yes Yes	Yes Yes

Figure 1 Study design. **A:** Flowchart of study subjects selected for blood proteomic profiling in the at-risk, acute respiratory distress syndrome (ARDS), and recovery cohorts. **B:** Venn diagram showing the overlap among subjects with COVID-19 across the study cohorts. **C:** Conceptual schematic of study subject sampling in relation to hospital admission (at-risk cohort), intensive care unit (ICU) admission (ARDS cohort), and ICU discharge (recovery cohort). **D:** Characteristics of study cohorts, including total subjects (*N*), blood sample type, existence of longitudinal samples, sample timing, and whether proteomic profiling, angiopoietin 2 (ANGPT2), and receptor-interacting protein kinase 3 (RIPK3) measurements were performed.

First, the vascular protein set was investigated only in subjects with COVID-19 ARDS (Supplemental Figure S4A). Protein results from the COVID-19 at-risk cohort were confirmed and low mean protein abundance of the protein set was associated with worse survival ($P = 0.026$) (Supplemental Figure S4B), low platelet count ($P < 0.001$) (Supplemental Figure S4C), and older patient age ($P = 0.035$) (Supplemental Figure S4D). The addition of non−COVID-19 ARDS patients (bacterial sepsis and influenza ARDS) led to a similar trend (Figure 3A), with survival ($P = 0.020$) (Figure 3B) and low platelets ($P < 0.001$) (Supplemental Figure S5A) associated with the low mean vascular protein abundance cluster ($P < 0.001$) (Supplemental Figure S5B). Age was not associated with low mean vascular protein abundance in this ARDS cohort ($P = 0.180$) (Supplemental Figure S5C). Similar to the at-risk cohort, baseline cancer status ($P < 0.001$) (Supplemental Table S3) and elevated baseline creatinine ($P = 0.022$) (Supplemental Table S3) were more frequent in ARDS subjects in the low mean vascular protein abundance cluster. More importantly, this low abundance signature did not reflect the relative expression of these proteins compared with healthy controls. As an example, CD40LG and ANGPT1 had opposite expression patterns in ARDS compared with healthy controls. Whereas CD40LG increased in ARDS compared with healthy control

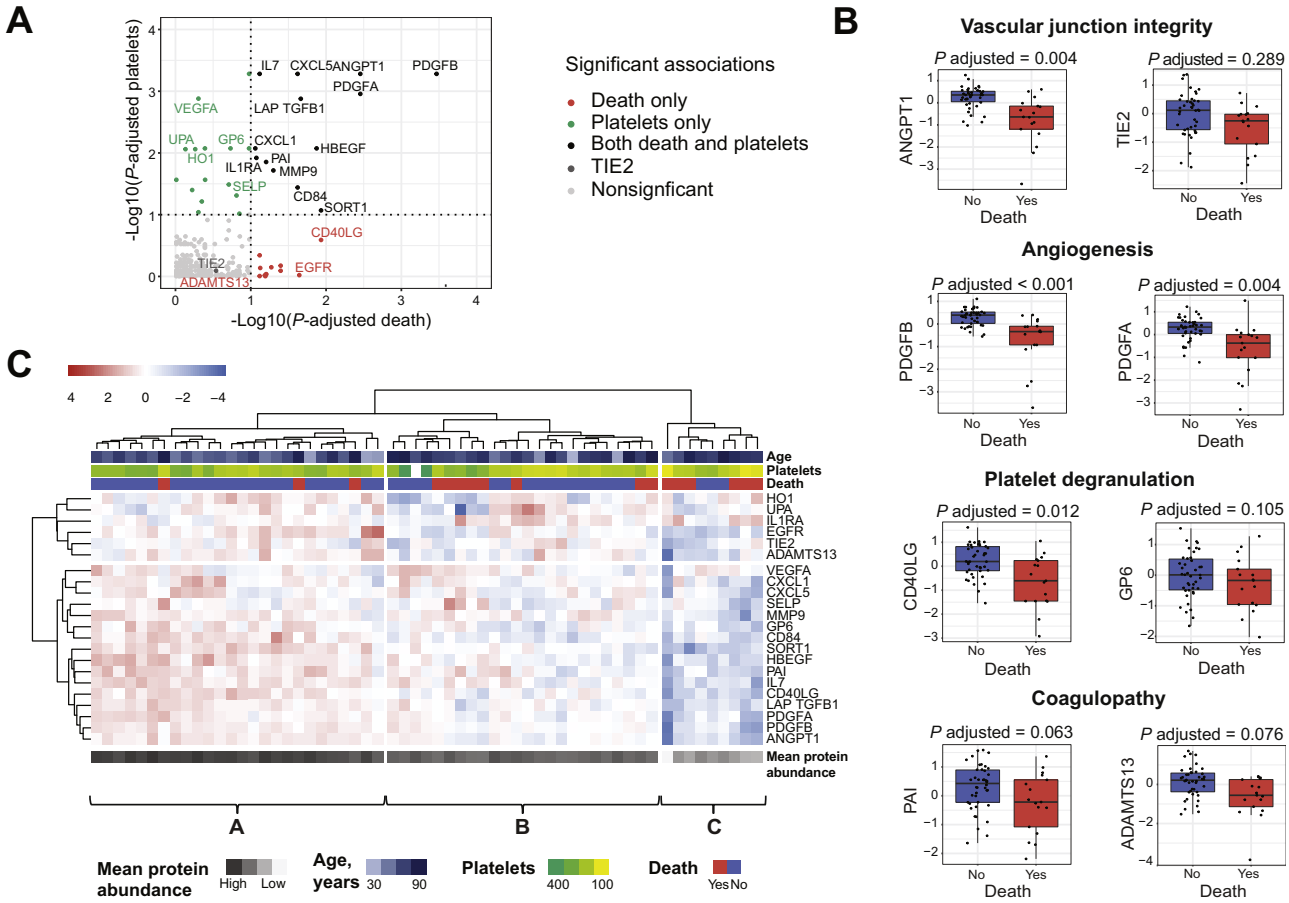

Figure 2 The hospitalized at-risk cohort blood proteome identifies a signature of vascular limitation preceding critical illness. **A:** Overview of the associations of the protein set to death and platelets. All displayed proteins were included in the final protein set. Proteins in green associated with platelets, proteins in red associated with death, and proteins in black associated with both. TIE2 was additionally included as it is the receptor for angiopoietin (ANGPT) 1 and ANGPT2. **B:** Box plots demonstrating the association between proteins of vascular junctional integrity, angiogenesis, platelet degranulation, and coagulopathy to mortality in the at-risk cohort after adjusting for multiple comparisons. Boxes indicate the interquartile range (IQR) of the data distribution, the **line** in the box represents the median value, and the whiskers extend for 1.5 times the range of the IQR. Dots indicate the protein level in individual patients. **C:** Heat map of protein set abundance in the at-risk COVID-19 subjects. Hierarchical clustering was performed using Ward linkage and euclidean distance. Age, platelet count, and death are overlaid at the top. Mean abundance of the 22-protein set is displayed at the bottom. Mean protein abundance is progressively lower from cluster A to B to C. $N = 59$ (**A**–**C**).

(Supplemental Figure S1C), ANGPT1 expression was similar to healthy control (Supplemental Figure S1D). Despite the opposite expression patterns of the ARDS biomarkers compared with healthy controls, lower expression of both CD40LG and ANGPT1 was associated with the low platelet, worse clinical outcomes cluster.

Similar to the at-risk cohort, the junctional integrity proteins ANGPT1 and TIE2 had lower expression in the low platelet, high mortality cluster B (Figure 3A). As ANGPT2 is known to negatively regulate ANGPT1 and TIE2, plasma ANGPT2 was measured in the ARDS cohort. Notably, plasma ANGPT2 was higher in the low mean protein abundance cluster ($P = 0.001$) (Figure 3C and Supplemental Figure S4E), linking low vascular protein abundance and plasma ANGPT2 in diverse ARDS subjects.

Interestingly, when COVID-19 ARDS was considered alone (Supplemental Figure S4), this higher vascular injury signature was present in 39% (12 of 31) of subjects with COVID-19 ARDS. However, when all three infection types were considered (Figure 3), only 13% (4 of 31) of subjects with COVID-19 ARDS were in the higher vascular injury cluster compared with 58% (14 of 24) of subjects with bacterial sepsis ARDS and 80% (3 of 4) of subjects with influenza ARDS. This demonstrated that COVID-19 ARDS may be associated with less ANGPT2-associated vascular injury than bacterial sepsis and influenza-related ARDS. This finding is supported by a lower ventilator ratio in subjects with COVID-19 ARDS compared with non–COVID-19 ARDS subjects (Supplemental Table S2), a physiological surrogate for vascular injury in ARDS.[30] This is also consistent with previous investigations showing higher platelet counts and less platelet consumption in COVID-19 compared with bacterial sepsis ARDS.[31]

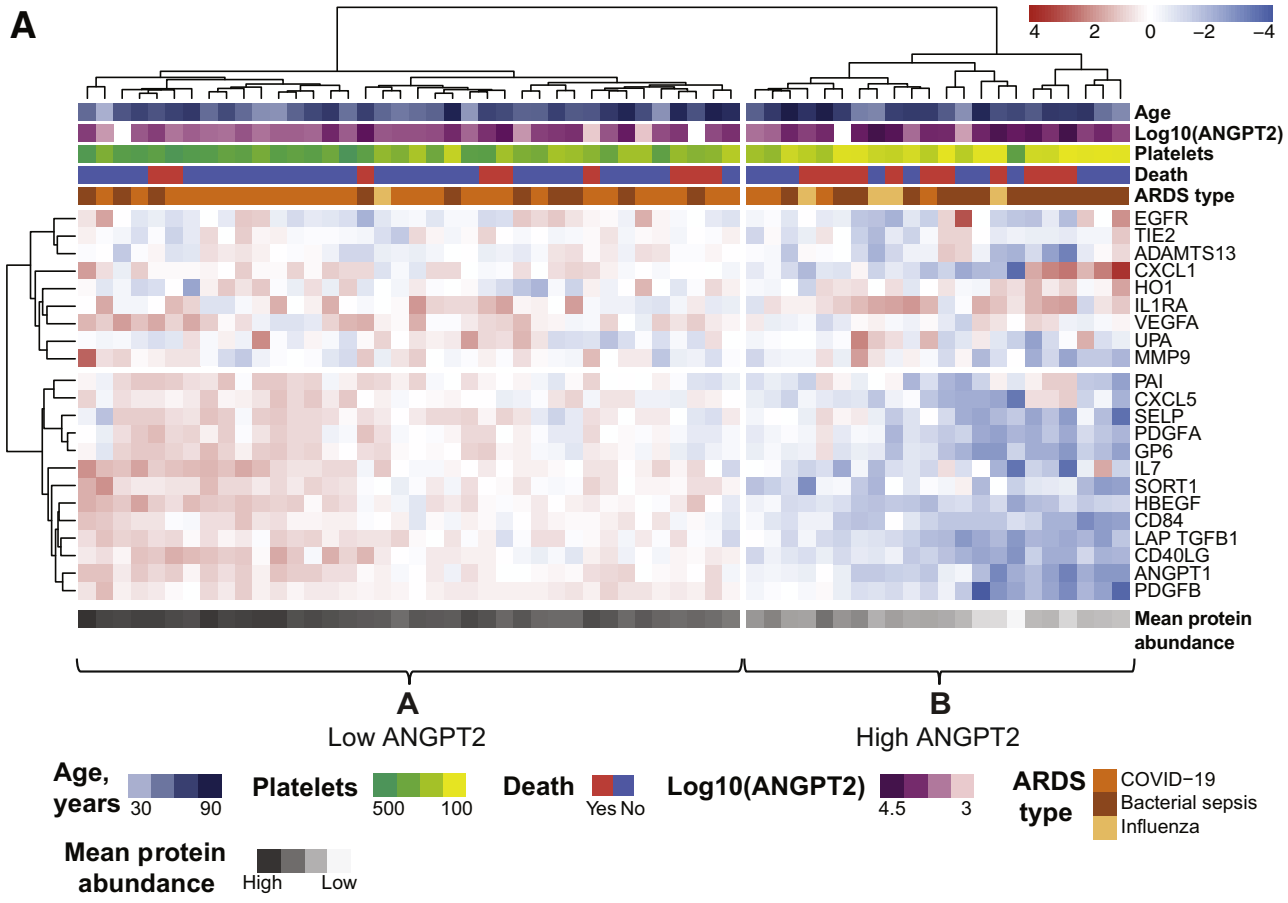

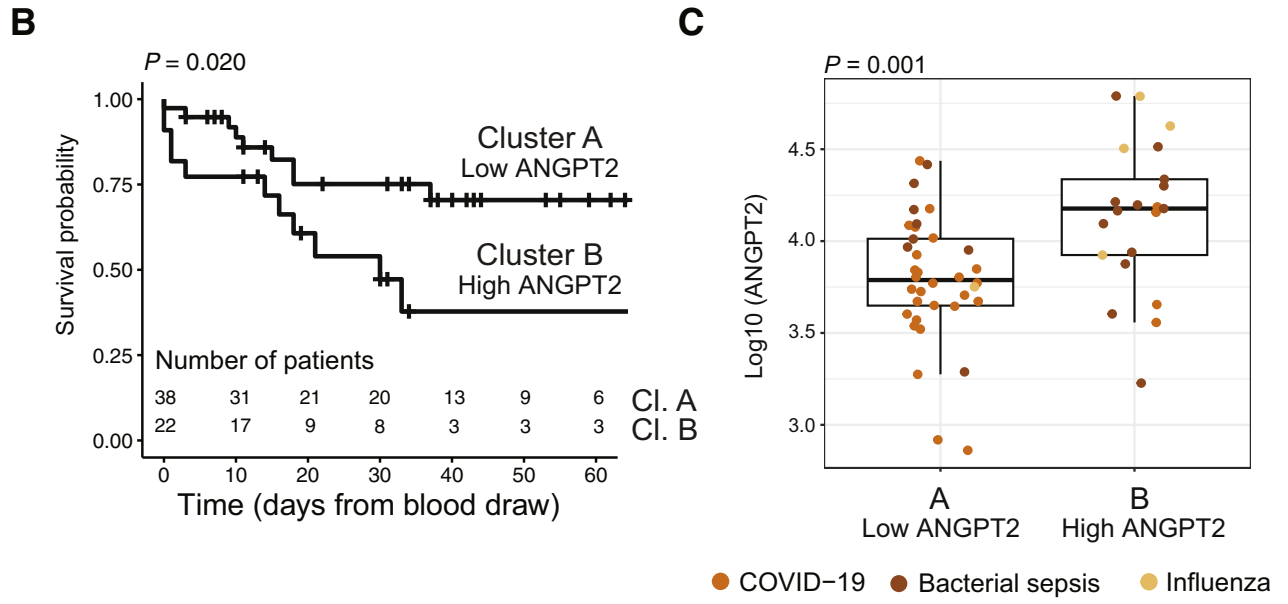

Figure 3 Loss of circulating vascular proteins is associated with low platelets, mortality, and plasma angiopoietin 2 (ANGPT2) in the acute respiratory distress syndrome (ARDS) cohort. **A:** Heat map of 22-protein set abundance in diverse ARDS subjects, divided into two clusters. Hierarchical clustering was performed using Ward linkage and euclidean distance. Age, log10(ANGPT2), platelet count, mortality, and ARDS etiology are overlayed at the top. Mean protein abundance of the 22-protein set is overlayed at the bottom. **B:** Kaplan-Meier survival analysis for the two heat map clusters showing worse survival for the high ANGPT2 ARDS cluster B. The *x* axis was capped at 60 days. The table at the bottom indicates the number of patients at risk at each time point in the two clusters. **C:** Log10(ANGPT2) values in the two clusters, demonstrating higher ANGPT2 expression in low vascular protein abundance cluster B. Differential statistic was assessed with a two-sided *U*-test. The boxes indicate the interquartile range (IQR) of the data distribution, the **line** in the box represents the median value, and the whiskers extend for 1.5 times the range of the IQR. Dots indicate the protein level in individual patients across the different ARDS categories: COVID-19 (**orange**), bacterial sepsis (**brown**), and influenza (**yellow**). $N = 60$ (**A**–**C**).

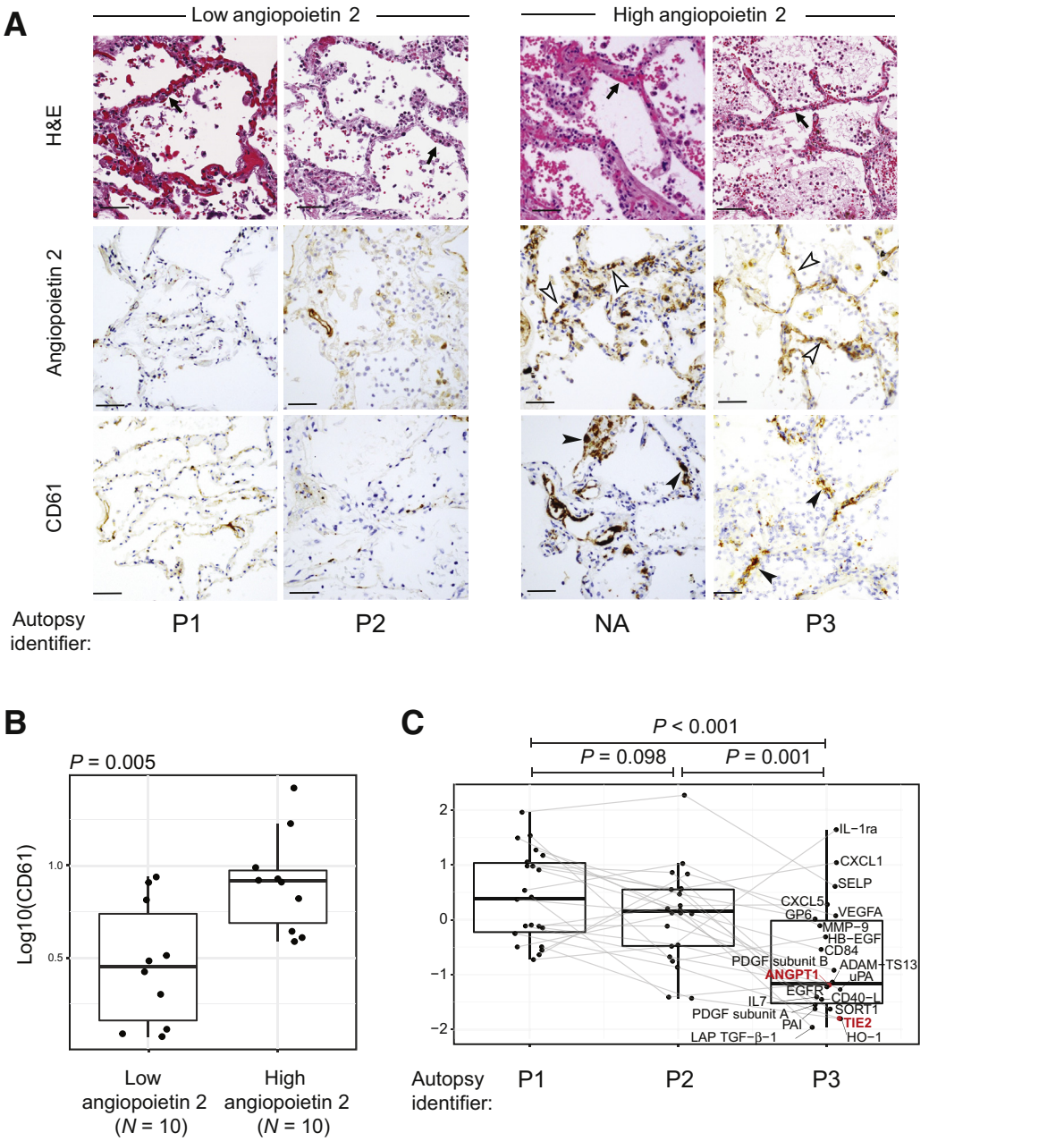

Figure 4 Angiopoietin 2 (ANGPT2) is correlated with CD61 staining microthrombi in subjects with COVID-19 acute respiratory distress syndrome (ARDS). **A:** Representative hematoxylin and eosin (H&E), ANGPT2, and CD61 staining in subjects with COVID-19 ARDS. H&E demonstrates alveolar septal wall thickening across displayed autopsy subjects (**arrows**). Increased ANGPT2 (**open arrowheads**) and CD61 (**closed arrowheads**) immunostaining is seen in subjects NA and P3 in a vascular distribution. **B:** Lung autopsy specimens from 20 subjects with COVID-19 ARDS were stained for ANGPT2 and platelet activation stain CD61. High ANGPT2 corresponds to autopsy subjects with ANGPT2 quantification above the median of the autopsy cohort, whereas low ANGPT2 represents the low ANGPT2 cohort. High ANGPT2 was associated with increased CD61 staining ($P = 0.005$). **C:** Blood proteomic data from autopsy subjects P1 and P2 (both low ANGPT2/low CD61 staining) and subject P3 (high ANGPT2 and high CD61) demonstrate that low expression of the vascular protein set is associated with high ANGPT2 and high CD61 staining. Angiopoietin axis proteins ANGPT1 and TIE2 highlighted in red. $N = 10$ for high ANGPT2 and $N = 10$ for low ANGPT2 (**B**). Scale bars = 50 μm (**A**). NA, no blood proteomic data available for the autopsy subject.

Angiopoietin 2 Correlates with CD61 Staining Microthrombi in Subjects with COVID-19 ARDS

The observed link between platelet activation and ANGPT2 was then explored in COVID-19 ARDS lung tissue. Twenty COVID-19 ARDS lung autopsy specimens were stained for the lung injury marker ANGPT2 and the activated platelet stain CD61. Representative sections from a high and low ANGPT2 subject are shown in Figure 4A. ANGPT2 staining was pronounced in the microvasculature and was mirrored by CD61-positive microthrombi in a similar distribution, linking vascular injury and platelet-rich

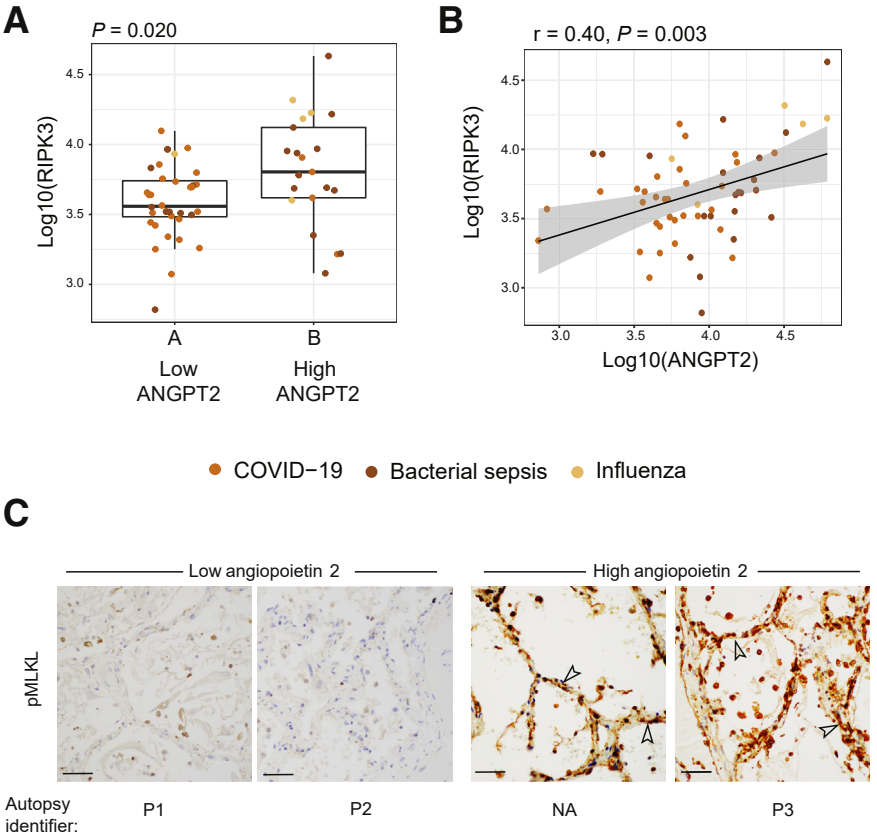

Figure 5 Induction of vascular cell death in angiopoietin 2 (ANGPT2)—associated vascular injury. **A:** Plasma receptor-interacting protein kinase 3 (RIPK3) in acute respiratory distress syndrome (ARDS) by heat map cluster (Figure 3A). RIPK3 is associated with high ANGPT2 ($P = 0.020$). COVID-19 (orange), bacterial sepsis (brown), and influenza (mustard) data are shown. **B:** Correlation of plasma RIPK3 and plasma ANGPT2 in the ARDS cohort (Figure 3). r indicates the Pearson correlation coefficient of the two variables, and *P* indicates its corresponding *P* value. The **black line** represents the linear regression line, and the gray area indicates the 95% CI of the fit. Dots indicate the protein level in individual patients across the different ARDS categories. **C:** Phosphorylated mixed lineage kinase domain-like (pMLKL) staining in COVID-19 ARDS autopsy subjects P1 and P2 (both low ANGPT2/low CD61 staining) and subjects NA and P3 (high ANGPT2 and high CD61), demonstrating increased expression of pMLKL (**open arrowheads**) in autopsy subjects with high ANGPT2 staining. $N = 60$ (**A** and **B**). Scale bars = 50 μm (**C**). NA, no blood proteomic data available for the autopsy subject.

microvascular microthrombi in COVID-19 ARDS. ANGPT2 and endothelial nuclear stain ERG costaining confirmed endothelial origin of the ANGPT2 staining (Supplemental Figure S6A). More importantly, staining for CD31 as a constitutive endothelial marker (Supplemental Figure S6B) showed that differences in ANGPT2 and CD61 staining in these subjects were not due to differences in preservation of endothelium between autopsy subjects. Quantification of ANGPT2 and CD61 staining showed that high ANGPT2 protein was associated with increased CD61 ($P = 0.005$) (Figure 4B). Blood proteomics was performed in three of the autopsy subjects (Figure 4, A and C) (subjects labeled as P1, P2, and P3). Consistent with the ARDS cohort, low protein abundance of the protein set, including lower expression of angiopoietin axis proteins ANGPT1 and TIE2 (Figure 4C), was associated with increased vascular ANGPT2 staining (Figure 4A).

Induction of Vascular Cell Death in ANGPT-2—Associated Vascular Injury

Having validated the vascular injury signature in diverse ARDS populations and COVID-19 ARDS autopsy tissue, whether ANGPT2-associated vascular injury could be associated with genetically regulated necrotic cell death, known as necroptosis, was investigated next. Increased expression of plasma RIPK3, a vital necroptosis protein,[32] was first demonstrated in subjects with high ANGPT2 ARDS ($P = 0.020$) (Figure 5A). Plasma RIPK3 was also correlated with plasma ANGPT2 ($r = 0.40$; $P = 0.003$) (Figure 5B), supporting the existence of a link between circulating necroptosis proteins and ANGPT2-associated vascular injury. Autopsy subjects with high ANGPT2 staining/low vascular protein abundance (Figure 4A) (NA and P3) demonstrated diffuse microvascular staining for pMLKL, a terminal protein in necrotic cell death execution downstream of RIPK3 (Figure 5C). Conversely, autopsy subjects with low ANGPT2 staining/high vascular protein abundance (Figure 4A) (P1 and P2) were negative for pMLKL. Taken together, these data link ANGPT2-associated vascular injury to necroptosis induction in COVID-19 ARDS.

Among Subjects with COVID-19 ARDS Recovery, Longitudinal Plasma Proteomics Identifies a Stable Protein Trajectory Associated with Good Functional Recovery

The 22-protein set was further investigated with respect to its predictive ability during COVID-19 ARDS recovery. Among 276 recovery subjects during the study period, 12

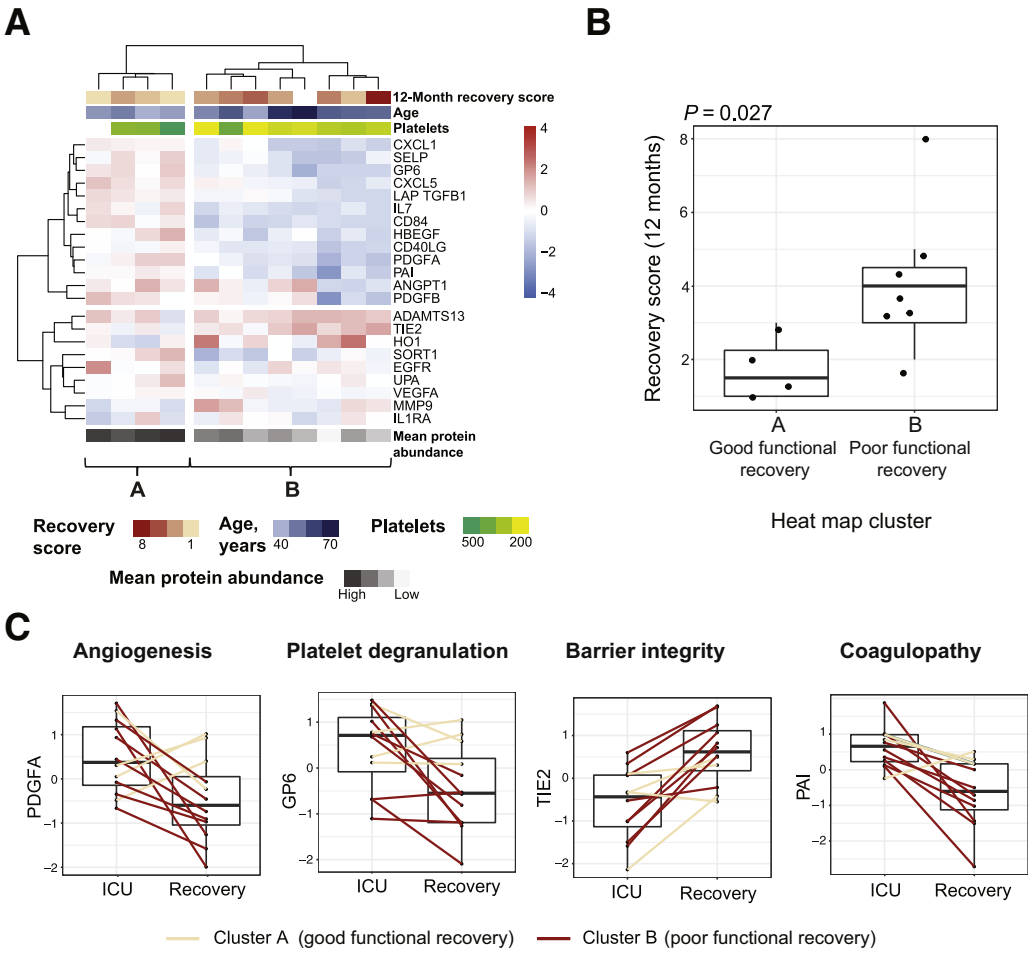

Figure 6 Among subjects with COVID-19 acute respiratory distress syndrome recovery, longitudinal plasma proteomics identifies a stable protein trajectory associated with good functional recovery. **A:** Heat map of COVID-19 recovery subjects. Functional recovery, age, platelet count, and 12-month recovery scores are overlaid at the top. Hierarchical clustering was performed with Ward linkage and euclidean distance. **B:** Follow-up recovery scores at 12 months after intensive care unit (ICU) admission in the two heat map clusters. Differential statistic was assessed with a two-sided *U*-test. The boxes indicate the interquartile range (IQR) of the data distribution, the **line** in the box represents the median value, and the whiskers extend for 1.5 times the range of the IQR. Dots indicate the protein level in individual patients. High scores indicate worse functional recovery. **C:** Trajectory of vascular proteins from ICU to recovery time points by functional recovery group. The boxes indicate the IQR of the data distribution, the **line** in the box represents the median value, and the whiskers extend for 1.5 times the range of the IQR. Dots indicate the protein level in individual patients in the two time points. Values from the same patient are linked by a **line** and colored according to the corresponding heat map cluster: A (**cream**) or B (**red**). Differential statistic of the protein trajectories between the two patient clusters was computed with a linear model. All displayed trajectory differences were significant to an adjusted $P < 0.25$. $N = 12$ (**A**–**C**).

subjects with COVID-19 ARDS had plasma available from both their ICU and recovery time point and were profiled longitudinally (Figure 1). Profiled recovery subjects were younger (47 versus 62 years old; $P = 0.002$) than unprofiled recovery subjects (Supplemental Table S1). The median age of profiled recovery cohort was 47 years, and was majority male (67% versus 33% female) (Supplemental Table S2).

Patient clustering based on the recovery plasma protein set revealed two distinct clusters (Figure 6A). Again, the low protein abundance cluster was associated with platelet level ($P = 0.048$) (Supplemental Figure S7A) and older age ($P = 0.048$) (Supplemental Figure S7B) but not ANGPT2 level ($P = 0.68$) (Supplemental Figure S7D). One-year follow-up functional recovery data based on the EQ-5D-3L questionnaire were available on 11 of these 12 recovery individuals (Figure 6A, see *Materials and Methods* for details). Notably, the cluster of patients with lower abundance of the protein set ($P = 0.004$) (Supplemental Figure S7C) displayed worse functional recovery 12 months after admission from the ICU, whereas higher vascular protein abundance was associated with better functional recovery ($P = 0.027$) (Figure 6B). To test whether the protein trajectory from ICU to recovery was different between good and poor functional recovery subjects, the differences in protein abundances was compared between the two time points in the two patient clusters (see *Materials and Methods*). For proteins representative of junctional barrier integrity (TIE2; $P = 0.20$), angiogenesis (PDGFA; $P = 0.20$), platelet degranulation (GP6; $P = 0.20$), and coagulopathy (PAI; $P = 0.20$), good functional recovery was associated with stable protein trajectory (Figure 6C), as opposed to the large

protein changes among the poor recovery subjects. This stable trajectory among good functional recovery subjects was similar for platelet levels ($P = 0.086$) (Supplemental Figure S7E) and ANGPT2 ($P = 0.083$) (Supplemental Figure S7F).

Discussion

This study traced a vascular protein signature through the natural history of COVID-19 ARDS from hospital admission to either recovery or death. As reflected in both the blood proteome and lung tissue, the clinical relevance of low abundance of circulating vascular proteins was demonstrated with known vascular functions and a link between ANGPT2 and vascular cell death, and in particular specialized necroptotic cell death, was revealed.

This vascular phenotype is notably present in certain subjects with COVID-19 before ICU admission. Although vascular injury spans the COVID-19 disease continuum from asymptomatic blue toes to catastrophic thromboembolic disease and ARDS-associated microangiopathy, the identification of broad loss of vascular protein expression in early severe disease generalizes this vascular dysfunction to the large population of hospitalized subjects with COVID-19. The loss of vascular proteins could result from SARS-CoV-2 endothelial infection.[6,7] However, this remains controversial and is thus far only reproducible in artificially engineered endothelial cells,[33] whereas primary human endothelial cells appear resistant to infection.[34] Alternatively, similar to bacterial sepsis[35,36] and influenza infection,[37] unrestrained COVID-19–related inflammatory signaling[13] was able to induce vascular cell death. Indeed, induction of genetically regulated necrotic cell death mediator (pMLKL) was demonstrated in the microvasculature of autopsy subjects with high ANGPT2-associated vascular injury COVID-19. Diverse upstream mediators previously linked to COVID-19 (eg, tumor necrosis factor-α[38] interferons[39,40]) can induce necroptosis,[32] providing a crucial link between SARS-CoV-2 infection and both direct (virus) or indirect (tumor necrosis factor and interferons) induction of vascular cell death in subjects with COVID-19. Vascular cell death in COVID-19 ARDS is also supported by lung imaging mass cytometry studies that show a reduction in the absolute number of endothelial cells in late COVID-19 autopsy tissue, which could reflect disease-related vascular cell death.[41]

The role of activated platelets in vascular injury and repair is also apparent in the data. Activated platelets amplify immune responses in early ARDS but also play an essential role in vascular repair. The consistently low platelet levels across the cohorts and the extensive microthrombi observed in the autopsy subjects imply a circulating milieu of platelet consumption. This milieu is supported by a blood signature of ongoing thrombolysis (high UPA and low PAI) and low levels of platelet-derived proteins (low SELP and GP6) in subjects with high ANGPT2-associated vascular injury. Relative loss of ADAMTS13, linked to secondary microangiopathy in COVID-19,[42] is similarly deficient in the high ANGPT2 subjects, linking platelet consumption with microangiopathy in severe COVID-19. Low platelets have previously been linked to ARDS mortality,[43] and the data suggest this may be related to depletion in platelet-related angiogenic[44–46] and junctional barrier factors.[47,48] Consistently low circulating angiogenic (low PDGFA and PDGFB) and barrier protein (low ANGPT1) in the higher ANGPT2 and low platelet subjects imply limitations in these essential reparative processes.

The validation of the vascular phenotype across diverse causes of ARDS broadens the relevance of the reported findings. In linking low platelets, vascular function, and mortality in COVID-19, bacterial sepsis, and influenza ARDS, the study hints at a common final pathway of vascular injury that is more disease- (ARDS) than cause- (COVID-19) specific. Matching COVID-19 and non–COVID-19 ARDS subjects would also have strengthened any comparison between these groups. However, the fact that there were similarities in protein expression despite stark differences in clinical parameters, including a marked difference in baseline cancer prevalence [14/29 (48%) in non–COVID-19 ARDS versus 1/31 (3%) in COVID-19 ARDS], remains a strength of the analysis as it suggests that different causes of platelet depletion (eg, failure of production in cancer patients with non–COVID-19 ARDS and consumption in COVID-19 ARDS patients) leads to the same protein expression pattern and worse clinical outcomes. Of note, this vascular injury pattern may be related to a reduced baseline vascular resilience in subjects with high ANGPT2-associated vascular injury. Consistently, subjects with high vascular injury are older,[49] have worse baseline renal function,[50,51] and are more likely to have cancer,[52] all variables known to be associated with vascular disease.

The identification of this severe vascular phenotype across infectious causes of ARDS also presents an opportunity for targeted vascular therapies in ARDS, including those that have shown promise in COVID-19,[53] in ARDS generally,[54] and in exciting preclinical[55,56] and early human experimental therapies, including a ANGPT1 supplementation trial in subjects with COVID-19 (*https://clinicaltrials.gov/ct2/show/NCT04737486*, last accessed March 5, 2022). Although an ANGPT2 neutralizing antibody study in hospitalized patients with COVID-19 was stopped for futility in October 2020 (*https://clinicaltrials.gov/ct2/show/NCT04342897*, last accessed March 5, 2022), the present data could improve patient selection for similar trials in the future, including the use of platelet levels to identify subjects with vascular limitation.

Finally, the identification of a vascular recovery proteome is novel. Nearly 4.5 million patients have been hospitalized in the United States since the start of the COVID-19 pandemic (*https://www.cdc.gov/coronavirus/2019-ncov/*

covid-data/covidview/index.html, last accessed March 5, 2022), with countless more hospitalized worldwide. However, even in recovery, patients remain at risk for disease-related morbidity and mortality.[57] This study demonstrated that a stable circulating vascular proteome is important for functional recovery. This association between vascular stability, platelet levels, and functional recovery could also support platelet levels as a novel biomarker in ARDS recovery. Larger studies will be needed to validate this observation.

This study has some limitations. Although a milieu of platelet consumption in subjects with ARDS and increased vascular injury was described here, alternative mechanisms of platelet depletion in these subjects, including decreased bone marrow production, particularly in the ARDS subjects with malignancies, cannot be ruled out. Platelet depletion also tracks with the vascular protein signature in the three cohorts, yet the study failed to establish cohort-specific platelet value that clinicians can use to identify these subjects. Although endothelial cells, pericytes, and platelets represent the likely cellular origin of the vascular signature, the lack of spatial proteomic or transcriptomic data allows for the possibility that some identified proteins are from nonvascular sources, including immune cells.[58] Future murine cell-specific knockout studies will be needed to resolve the cellular origin of the signature. Finally, although an association between ANGPT2, vascular cell death proteins RIPK3, and pMLKL was observed, additional *in vivo* and *in vitro* studies will be needed to determine the critical cross talk between vascular injury and vascular cell death proteins.

In summary, this study identified a vascular injury signal in COVID-19 ARDS that has predictive value in early disease through recovery as well as in bacterial sepsis and influenza ARDS. This signal was able to improve patient selection and timing of vascular targeted therapies in ARDS.

Acknowledgment

We thank Ilias I. Siempos for critically reviewing the article.

Author Contributions

D.R.P. and E.B. share first authorship; D.R.P. is listed first based on higher total effort to the project. D.R.P., E.B., J.K., A.M.K.C., and S.R. designed the study; D.R.P., A.C.R., and A.C.B. performed the autopsy staining analyses; L.G.-E., S.A.-M., A.C., C.N.P., A.R., J.G.C., and S.Z.J. processed samples and organized the patient clinical data; E.B., H.S., R.B., M.B., K.C., F.S., and J.K. analyzed the proteomic data; K.L.H. and I.E. provided statistical support for patient clinical data; E.L., K.W., C.N.P., and L.L. performed functional assessment of recovery subjects; D.R.P., E.B., J.K., A.M.K.C., R.B., F.S., J.G.C., E.J.S., A.C.R., H.O.R., J.L., M.E.C., and S.R. critically appraised the final data set; D.R.P. and E.B. wrote the article. All authors approved the final article.

Supplemental Data

Supplemental material for this article can be found at *http://doi.org/10.1016/j.ajpath.2022.04.002*.

References

1. Matthay MA, Zemans RL, Zimmerman GA, Arabi YM, Beitler JR, Mercat A, Herridge M, Randolph AG, Calfee CS: Acute respiratory distress syndrome. Nat Rev Dis Primers 2019, 5:18
2. Meyer NJ, Calfee CS: Novel translational approaches to the search for precision therapies for acute respiratory distress syndrome. Lancet Respir Med 2017, 5:512–523
3. Agrawal A, Matthay MA, Kangelaris KN, Stein J, Chu JC, Imp BM, Cortez A, Abbott J, Liu KD, Calfee CS: Plasma angiopoietin-2 predicts the onset of acute lung injury in critically ill patients. Am J Respir Crit Care Med 2013, 187:736–742
4. Gallagher DC, Parikh SM, Balonov K, Miller A, Gautam S, Talmor D, Sukhatme VP: Circulating angiopoietin 2 correlates with mortality in a surgical population with acute lung injury/adult respiratory distress syndrome. Shock 2008, 29:656–661
5. Ziegler T, Horstkotte J, Schwab C, Pfetsch V, Weinmann K, Dietzel S, Rohwedder I, Hinkel R, Gross L, Lee S, Hu J, Soehnlein O, Franz WM, Sperandio M, Pohl U, Thomas M, Weber C, Augustin HG, Fässler R, Deutsch U, Kupatt C: Angiopoietin 2 mediates microvascular and hemodynamic alterations in sepsis. J Clin Invest 2013, 123:3436–3445
6. Ackermann M, Verleden SE, Kuehnel M, Haverich A, Welte T, Laenger F, Vanstapel A, Werlein C, Stark H, Tzankov A, Li WW, Li VW, Mentzer SJ, Jonigk D: Pulmonary vascular endothelialitis, thrombosis, and angiogenesis in Covid-19. N Engl J Med 2020, 383:120–128
7. Varga Z, Flammer AJ, Steiger P, Haberecker M, Andermatt R, Zinkernagel AS, Mehra MR, Schuepbach RA, Ruschitzka F, Moch H: Endothelial cell infection and endotheliitis in COVID-19. Lancet 2020, 395:1417–1418
8. Bradley BT, Maioli H, Johnston R, Chaudhry I, Fink SL, Xu H, Najafian B, Deutsch G, Lacy JM, Williams T, Yarid N, Marshall DA: Histopathology and ultrastructural findings of fatal COVID-19 infections in Washington State: a case series. Lancet 2020, 396: 320–332
9. Magro C, Mulvey JJ, Berlin D, Nuovo G, Salvatore S, Harp J, Baxter-Stoltzfus A, Laurence J: Complement associated microvascular injury and thrombosis in the pathogenesis of severe COVID-19 infection: a report of five cases. Transl Res 2020, 220:1–13
10. Borczuk AC, Salvatore SP, Seshan SV, Patel SS, Bussel JB, Mostyka M, Elsoukkary S, He B, Del Vecchio C, Fortarezza F, Pezzuto F, Navalesi P, Crisanti A, Fowkes ME, Bryce CH, Calabrese F, Beasley MB: COVID-19 pulmonary pathology: a multi-institutional autopsy cohort from Italy and New York City. Mod Pathol 2020, 33:2156–2168
11. Choi JJ, Wehmeyer GT, Li HA, Alshak MN, Nahid M, Rajan M, Liu B, Schatoff EM, Elahjji R, Abdelghany Y, D'Angelo D, Crossman D, Evans AT, Steel P, Pinheiro LC, Goyal P, Safford MM, Mints G, DeSancho MT: D-dimer cut-off points and risk of venous thromboembolism in adult hospitalized patients with COVID-19. Thromb Res 2020, 196:318–321
12. Jose RJ, Manuel A: COVID-19 cytokine storm: the interplay between inflammation and coagulation. Lancet Respir Med 2020, 8:e46–e47
13. Moore JB, June CH: Cytokine release syndrome in severe COVID-19. Science 2020, 368:473–474

14. Schmaier AA, Pajares Hurtado GM, Manickas-Hill ZJ, Sack KD, Chen SM, Bhambhani V, Quadir J, Nath AK, Collier A-RY, Ngo D, Barouch DH, Shapiro NI, Gerszten RE, Yu XG; MGH COVID-19 Collection and Processing Team, Peters KG, Flaumenhaft R, Parikh SM: Tie2 activation protects against prothrombotic endothelial dysfunction in COVID-19. JCI Insight 2021, 6:e151527
15. Schenck EJ, Ma KC, Price DR, Nicholson T, Oromendia C, Gentzler ER, Sanchez E, Baron RM, Fredenburgh LE, Huh J-W, Siempos II, Choi AM: Circulating cell death biomarker TRAIL is associated with increased organ dysfunction in sepsis. JCI Insight 2019, 4:e127143
16. Ma KC, Schenck EJ, Siempos II, Cloonan SM, Finkelsztein EJ, Pabon MA, Oromendia C, Ballman KV, Baron RM, Fredenburgh LE, Higuera A, Lee JY, Chung CR, Jeon K, Yang JH, Howrylak JA, Huh J-W, Suh GY, Choi AM: Circulating RIPK3 levels are associated with mortality and organ failure during critical illness. JCI Insight 2018, 3:e99692
17. Sureshbabu A, Patino E, Ma KC, Laursen K, Finkelsztein EJ, Akchurin O, Muthukumar T, Ryter SW, Gudas L, Choi AMK, Choi ME: RIPK3 promotes sepsis-induced acute kidney injury via mitochondrial dysfunction. JCI Insight 2018, 3:e98411
18. Siempos II, Ma KC, Imamura M, Baron RM, Fredenburgh LE, Huh J-W, Moon J-S, Finkelsztein EJ, Jones DS, Lizardi MT, Schenck EJ, Ryter SW, Nakahira K, Choi AM: RIPK3 mediates pathogenesis of experimental ventilator-induced lung injury. JCI Insight 2018, 3:e97102
19. Schenck EJ, Hoffman K, Goyal P, Choi J, Torres L, Rajwani K, Tam CW, Ivascu N, Martinez FJ, Berlin DA: Respiratory mechanics and gas exchange in COVID-19-associated respiratory failure. Ann Am Thorac Soc 2020, 17:1158−1161
20. Price DR, Hoffman KL, Oromendia C, Torres LK, Schenck EJ, Choi ME, Choi AMK, Baron RM, Huh J-W, Siempos II: Effect of neutropenic critical illness on development and prognosis of acute respiratory distress syndrome. Am J Respir Crit Care Med 2021, 203: 504−508
21. Vincent JL, Moreno R, Takala J, Willatts S, De Mendonça A, Bruining H, Reinhart CK, Suter PM, Thijs LG; on behalf of the Working Group on Sepsis-Related Problems of the European Society of Intensive Care Medicine: The SOFA (Sepsis-related Organ Failure Assessment) score to describe organ dysfunction/failure. Intensive Care Med 1996, 22:707−710
22. ARDS Definition Task Force, Ranieri VM, Rubenfeld GD, Thompson BT, Ferguson ND, Caldwell E, Fan E, Camporota L, Slutsky AS: Acute respiratory distress syndrome: the Berlin definition. JAMA 2012, 307:2526−2533
23. Devlin NJ, Brooks R: EQ-5D and the EuroQol Group: past, present and future. Appl Health Econ Health Policy 2017, 15:127−137
24. Varghese F, Bukhari AB, Malhotra R, De A: IHC Profiler: an open source plugin for the quantitative evaluation and automated scoring of immunohistochemistry images of human tissue samples. PLoS One 2014, 9:e96801
25. Dieterle F, Ross A, Schlotterbeck G, Senn H: Probabilistic quotient normalization as robust method to account for dilution of complex biological mixtures: application in 1H NMR metabonomics. Anal Chem 2006, 78:4281−4290
26. Do KT, Wahl S, Raffler J, Molnos S, Laimighofer M, Adamski J, Suhre K, Strauch K, Peters A, Gieger C, Langenberg C, Stewart ID, Theis FJ, Grallert H, Kastenmüller G, Krumsiek J: Characterization of missing values in untargeted MS-based metabolomics data and evaluation of missing data handling strategies. Metabolomics 2018, 14:128
27. Benjamini Y, Hochberg Y: Controlling the false discovery rate: a practical and powerful approach to multiple testing. J R Stat Soc Ser B Methodol 1995, 57:289−300
28. Chetnik K, Benedetti E, Gomari DP, Schweickart A, Batra R, Buyukozkan M, Wang Z, Arnold M, Zierer J, Suhre K, Krumsiek J: maplet: An extensible R toolbox for modular and reproducible metabolomics pipelines. Bioinformatics 2021, 38:1168−1170
29. Kim M, Allen B, Korhonen EA, Nitschké M, Yang HW, Baluk P, Saharinen P, Alitalo K, Daly C, Thurston G, McDonald DM: Opposing actions of angiopoietin-2 on Tie2 signaling and FOXO1 activation. J Clin Invest 2016, 126:3511−3525
30. Morales-Quinteros L, Schultz MJ, Bringué J, Calfee CS, Camprubí M, Cremer OL, Horn J, van der Poll T, Sinha P, Artigas A, Bos LD; MARS Consortium: Estimated dead space fraction and the ventilatory ratio are associated with mortality in early ARDS. Ann Intensive Care 2019, 9:128
31. Helms J, Tacquard C, Severac F, Leonard-Lorant I, Ohana M, Delabranche X, Merdji H, Clere-Jehl R, Schenck M, Fagot Gandet F, Fafi-Kremer S, Castelain V, Schneider F, Grunebaum L, Anglés-Cano E, Sattler L, Mertes P-M, Meziani F; CRICS TRIGGERSEP Group (Clinical Research in Intensive Care and Sepsis Trial Group for Global Evaluation and Research in Sepsis): High risk of thrombosis in patients with severe SARS-CoV-2 infection: a multicenter prospective cohort study. Intensive Care Med 2020, 46:1089−1098
32. Choi ME, Price DR, Ryter SW, Choi AMK: Necroptosis: a crucial pathogenic mediator of human disease. JCI Insight 2019, 4: e128834
33. Monteil V, Kwon H, Prado P, Hagelkrüys A, Wimmer RA, Stahl M, Leopoldi A, Garreta E, Hurtado Del Pozo C, Prosper F, Romero JP, Wirnsberger G, Zhang H, Slutsky AS, Conder R, Montserrat N, Mirazimi A, Penninger JM: Inhibition of SARS-CoV-2 infections in engineered human tissues using clinical-grade soluble human ACE2. Cell 2020, 181:905−913.e7
34. Ahmetaj-Shala B, Peacock TP, Baillon L, Swann O, Gashaw H, Barclay WS, Mitchell JA: Resistance of endothelial cells to SARS-CoV-2 infection in vitro. bioRxiv 2020. [Preprint] doi: 10.1101/2020.11.08.372581
35. Zelic M, Roderick JE, O'Donnell JA, Lehman J, Lim SE, Janardhan HP, Trivedi CM, Pasparakis M, Kelliher MA: RIP kinase 1-dependent endothelial necroptosis underlies systemic inflammatory response syndrome. J Clin Invest 2018, 128:2064−2075
36. Najjar M, Saleh D, Zelic M, Nogusa S, Shah S, Tai A, Finger JN, Polykratis A, Gough PJ, Bertin J, Whalen M, Pasparakis M, Balachandran S, Kelliher M, Poltorak A, Degterev A: RIPK1 and RIPK3 kinases promote cell-death-independent inflammation by toll-like receptor 4. Immunity 2016, 45:46−59
37. Shubina M, Tummers B, Boyd DF, Zhang T, Yin C, Gautam A, Guo X-ZJ, Rodriguez DA, Kaiser WJ, Vogel P, Green DR, Thomas PG, Balachandran S: Necroptosis restricts influenza A virus as a stand-alone cell death mechanism. J Exp Med 2020, 217: e20191259
38. Del Valle DM, Kim-Schulze S, Huang H-H, Beckmann ND, Nirenberg S, Wang B, Lavin Y, Swartz TH, Madduri D, Stock A, Marron TU, Xie H, Patel M, Tuballes K, Van Oekelen O, Rahman A, Kovatch P, Aberg JA, Schadt E, Jagannath S, Mazumdar M, Charney AW, Firpo-Betancourt A, Mendu DR, Jhang J, Reich D, Sigel K, Cordon-Cardo C, Feldmann M, Parekh S, Merad M, Gnjatic S: An inflammatory cytokine signature predicts COVID-19 severity and survival. Nat Med 2020, 26:1636−1643
39. Hadjadj J, Yatim N, Barnabei L, Corneau A, Boussier J, Smith N, Péré H, Charbit B, Bondet V, Chenevier-Gobeaux C, Breillat P, Carlier N, Gauzit R, Morbieu C, Pène F, Marin N, Roche N, Szwebel T-A, Merkling SH, Treluyer J-M, Veyer D, Mouthon L, Blanc C, Tharaux P-L, Rozenberg F, Fischer A, Duffy D, Rieux-Laucat F, Kernéis S, Terrier B: Impaired type I interferon activity and inflammatory responses in severe COVID-19 patients. Science 2020, 369:718−724
40. Lee JS, Park S, Jeong HW, Ahn JY, Choi SJ, Lee H, Choi B, Nam SK, Sa M, Kwon J-S, Jeong SJ, Lee HK, Park SH, Park S-H, Choi JY, Kim S-H, Jung I, Shin E-C: Immunophenotyping of COVID-19 and influenza highlights the role of type I interferons in development of severe COVID-19. Sci Immunol 2020, 5:eabd1554
41. Rendeiro AF, Ravichandran H, Bram Y, Chandar V, Kim J, Meydan C, Park J, Foox J, Hether T, Warren S, Kim Y, Reeves J, Salvatore S, Mason CE, Swanson EC, Borczuk AC, Elemento O,

Schwartz RE: The spatial landscape of lung pathology during COVID-19 progression. Nature 2021, 593:564−569
42. Martinelli N, Montagnana M, Pizzolo F, Friso S, Salvagno GL, Forni GL, Gianesin B, Morandi M, Lunardi C, Lippi G, Polati E, Olivieri O, De Franceschi L: A relative ADAMTS13 deficiency supports the presence of a secondary microangiopathy in COVID 19. Thromb Res 2020, 193:170−172
43. Wang T, Liu Z, Wang Z, Duan M, Li G, Wang S, Li W, Zhu Z, Wei Y, Christiani DC, Li A, Zhu X: Thrombocytopenia is associated with acute respiratory distress syndrome mortality: an international study. PLoS One 2014, 9:e94124
44. Kisucka J, Butterfield CE, Duda DG, Eichenberger SC, Saffaripour S, Ware J, Ruggeri ZM, Jain RK, Folkman J, Wagner DD: Platelets and platelet adhesion support angiogenesis while preventing excessive hemorrhage. Proc Natl Acad Sci U S A 2006, 103: 855−860
45. Hall-Glenn F, De Young RA, Huang B-L, van Handel B, Hofmann JJ, Chen TT, Choi A, Ong JR, Benya PD, Mikkola H, Iruela-Arispe ML, Lyons KM: CCN2/connective tissue growth factor is essential for pericyte adhesion and endothelial basement membrane formation during angiogenesis. PLoS One 2012, 7:e30562
46. Lakka Klement G, Shai E, Varon D: The role of platelets in angiogenesis. Platelets. Cambridge, MA: Academic Press, 2013. pp. 487−502
47. Li JJ, Huang YQ, Basch R, Karpatkin S: Thrombin induces the release of angiopoietin-1 from platelets. Thromb Haemost 2001, 85: 204−206
48. Thurston G, Rudge JS, Ioffe E, Zhou H, Ross L, Croll SD, Glazer N, Holash J, McDonald DM, Yancopoulos GD: Angiopoietin-1 protects the adult vasculature against plasma leakage. Nat Med 2000, 6: 460−463
49. Savji N, Rockman CB, Skolnick AH, Guo Y, Adelman MA, Riles T, Berger JS: Association between advanced age and vascular disease in different arterial territories: a population database of over 3.6 million subjects. J Am Coll Cardiol 2013, 61:1736−1743
50. Anavekar NS, McMurray JJV, Velazquez EJ, Solomon SD, Kober L, Rouleau J-L, White HD, Nordlander R, Maggioni A, Dickstein K, Zelenkofske S, Leimberger JD, Califf RM, Pfeffer MA: Relation between renal dysfunction and cardiovascular outcomes after myocardial infarction. N Engl J Med 2004, 351:1285−1295
51. Wattanakit K, Folsom AR, Selvin E, Coresh J, Hirsch AT, Weatherley BD: Kidney function and risk of peripheral arterial disease: results from the Atherosclerosis Risk in Communities (ARIC) Study. J Am Soc Nephrol 2007, 18:629−636
52. Sturgeon KM, Deng L, Bluethmann SM, Zhou S, Trifiletti DM, Jiang C, Kelly SP, Zaorsky NG: A population-based study of cardiovascular disease mortality risk in US cancer patients. Eur Heart J 2019, 40:3889−3897
53. Gupta A, Madhavan MV, Poterucha TJ, DeFilippis EM, Hennessey JA, Redfors B, Eckhardt C, Bikdeli B, Platt J, Nalbandian A, Elias P, Cummings MJ, Nouri SN, Lawlor M, Ranard LS, Li J, Boyle C, Givens R, Brodie D, Krumholz HM, Stone GW, Sethi SS, Burkhoff D, Uriel N, Schwartz A, Leon MB, Kirtane AJ, Wan EY, Parikh SA: Association between antecedent statin use and decreased mortality in hospitalized patients with COVID-19. Nat Commun 2021, 12:1325
54. Sinha P, Delucchi KL, Thompson BT, McAuley DF, Matthay MA, Calfee CS; NHLBI ARDS Network: Latent class analysis of ARDS subphenotypes: a secondary analysis of the statins for acutely injured lungs from sepsis (SAILS) study. Intensive Care Med 2018, 44: 1859−1869
55. Schachterle W, Badwe CR, Palikuqi B, Kunar B, Ginsberg M, Lis R, Yokoyama M, Elemento O, Scandura JM, Rafii S: Sox17 drives functional engraftment of endothelium converted from non-vascular cells. Nat Commun 2017, 8:13963
56. Rafii S, Ginsberg M, Scandura J, Butler JM, Ding B-S: Transplantation of endothelial cells to mitigate acute and chronic radiation injury to vital organs. Radiat Res 2016, 186:196−202
57. Al-Aly Z, Xie Y, Bowe B: High-dimensional characterization of post-acute sequelae of COVID-19. Nature 2021, 594:259−264
58. Daamen AR, Bachali P, Owen KA, Kingsmore KM, Hubbard EL, Labonte AC, Robl R, Shrotri S, Grammer AC, Lipsky PE: Comprehensive transcriptomic analysis of COVID-19 blood, lung, and airway. Sci Rep 2021, 11:7052